

# ECG-EMG Separation by Using Enhanced Non-Negative Matrix Factorization

\*Maciej Niegowski and Miroslav Zivanovic

**Abstract** - We present a novel approach to single-channel ECG-EMG signal separation by means of enhanced non-negative matrix factorization (NMF). The approach is based on a linear decomposition of the input signal spectrogram in two non-negative components, which represent the ECG and EMG spectrogram estimates. As ECG and EMG have different time-frequency (TF) patterns, the decomposition is enhanced by reshaping the input mixture spectrogram in order to emphasize a sparse ECG over a noisy-like EMG. Moreover, initialization of the classical NMF algorithm with accurately designed ECG and EMG structures further increases its separation performance. The comparative study suggests that the proposed method outperforms two reference methods for both synthetic and real signal mixture scenarios.

## I. INTRODUCTION

The separation of ECG from single-channel surface EMG recordings remains an important task for a number of biomedical signal processing applications. The major difficulty arises from the fact that ECG and EMG simultaneously overlap in the time and frequency domain. This overlap is particularly significant in the 0.1 - 50 Hz band, where most of the ECG signal energy is clustered. Thus, ECG-EMG separation is a challenging task that requires an adequate approach.

A number of approaches can be identified from a vast literature in this field. The simplest one uses conventional high-pass filtering with a 4<sup>th</sup> order Butterworth filter with a cut-off frequency of 30 Hz [1]. The techniques based on adaptive filtering in general outperform the filtering approach at the expense of requiring additional ECG/EMG reference signals [2-4]. Adaptive filtering combined with wavelet analysis eliminates the need for external reference signals [5]. However, selection of proper wavelet shape and corresponding decision thresholds remain the key issue in the related methods. Let us also mention the statistical approach, e.g. independent component analysis (ICA) and its variants, which aim to separate linearly mixed statistically independent sources from multi-channel recordings [6].

In the present paper we propose a novel single-channel ECG-EMG separation approach based on the non-negative factorization of a TF signal representation (typically the spectrogram). This approach has successfully been used for

years in the image and audio signal processing domain for image deblurring and music quasi-harmonic source separation [7-9]. It has also been used in biomedicine for EEG classification [10] and multichannel EMG recognition [11] but, to the best of our knowledge, never for ECG-EMG separation.

The NMF approach, which operates on non-negative spectrograms, has proven to be very useful for discrimination of audio signals with significantly different TF behaviors [8, 9]. This means that it might be considered as a tool for the present application, given that EMG and ECG exhibit very different patterns in a spectrogram. Moreover, knowing that EMG can be regarded as a noise-like signal, whereas ECG has a time-variant harmonic structure, the following enhancements are incorporated into the classical NMF framework: 1) the spectrogram of the input signal is reshaped by low-pass filtering and decimation, which brings out the ECG TF patterns, and 2) the separation algorithm is initialized by carefully designed TF structures for both ECG and EMG signal components. The separation is carried out by iteratively minimizing a cost function which quantifies the difference between the original and estimated ECG and EMG spectrograms. Once the convergence of the algorithm is reached, the estimated ECG waveform is obtained by means of the inverse STFT.

The present paper is organized as follows. In Section 2 the NMF approach to ECG-EMG separation is presented. Section 3 contains results of a comparative study between three different approaches for both synthetic and real signals.

## II. METHOD

### A. NMF – General framework

NMF has been investigated by many researchers, but it has gained popularity through the works [12, 13]. In contrast to many unsupervised learning algorithms such as principal components analysis or ICA, it relies on non-negativity constraints. In order to apply NMF in biomedical scenarios, time domain signals need to be transformed into non-negative representations. The magnitude of the spectrogram of a given time domain signal meets the non-negativity requirement perfectly.

Let  $\mathbf{V}$  be a non-negative matrix  $\mathbf{V} \in \mathbb{R}^{\geq 0, M \times N}$ . The decomposition of  $\mathbf{V}$  can be done in such a way that the product of the resulting non-negative matrices  $\mathbf{W} \in \mathbb{R}^{\geq 0, M \times r}$  and  $\mathbf{H} \in \mathbb{R}^{\geq 0, r \times N}$  equals approximately matrix  $\mathbf{V}$ :

$$\mathbf{V} \approx \mathbf{WH} \quad (1)$$

*Asterisk indicates corresponding author.*

\*M. Niegowski is with the Electrical Engineering Department, Public University of Navarra, 31006 Pamplona, Spain (e-mail: maciej.niegowski@unavarra.es)

M. Zivanovic is with the Electrical Engineering Department, Public University of Navarra, 31006 Pamplona, Spain (e-mail: miro@unavarra.es)

Equation (1) can also be expressed in an alternative way:

$$\mathbf{V} \approx \sum_{r=1}^R w_r h_r, \quad (2)$$

where  $w_r$  and  $h_r$  represent the  $r^{\text{th}}$  column of  $\mathbf{W}$  and the  $r^{\text{th}}$  row of  $\mathbf{H}$  respectively. Factor  $r$  denotes the number of expected signal sources in the given input mixture. The source separation is performed by a decomposition of the spectrogram of the input signal and then by clustering these products into separate signal sources.

In a general NMF framework the matrices  $\mathbf{W}$  and  $\mathbf{H}$  are initialized with positive random entries and then alternatively updated with the following multiplicative update rules [13]:

$$\mathbf{W} \leftarrow \mathbf{W} \cdot (\mathbf{H}^T \mathbf{V}) ./ (\mathbf{H}^T \mathbf{H} \mathbf{W}), \quad (3)$$

$$\mathbf{H} \leftarrow \mathbf{H} \cdot (\mathbf{V} \mathbf{W}^T) ./ (\mathbf{H} \mathbf{W} \mathbf{W}^T), \quad (4)$$

where  $\cdot$  and  $./$  denote element-wise multiplication and division respectively. The reconstruction error between  $\mathbf{V}$  and the product  $\mathbf{W}\mathbf{H}$  is minimized, while constraining the matrices to be entry-wise non-negative. The quality of the reconstruction is measured by the cost function  $\mathbf{C}$ , which evaluates the square of the Euclidean distance between  $\mathbf{V}$  and  $\mathbf{W}\mathbf{H}$ :

$$\mathbf{C} = \|\mathbf{V} - \mathbf{W}\mathbf{H}\|^2 = \sum_{ij} (\mathbf{V}_{ij} - (\mathbf{W}\mathbf{H})_{ij})^2. \quad (5)$$

### B. Proposed methodology

The herein proposed enhanced NMF method, schematically represented in Fig.1, can be divided into three steps: (a) spectrogram reshaping, (b)  $\mathbf{W}$  and  $\mathbf{H}$  initialization and (c) NMF analysis. Each input signal is a single-channel record with concurrent ECG and EMG source signals.

*Step1.* The reshaping of the input spectrogram is performed in order to obtain clearer ECG patterns (Fig.1a). The light vertical lines at the bottom of the "Input TF" spectrogram belong to the ECG, whereas the EMG is represented by the blurry background. In order to emphasize the ECG patterns, we applied a 5<sup>th</sup> Butterworth LP filter with a cut-off frequency at 50 Hz to the input signal. Next, the signal was down-sampled at 100 Hz, with the decimation factor  $M$  coupled to the original sampling frequency. In the "Reshaped TF" spectrogram the ECG patterns are clearly enhanced.

*Step2.* The matrices  $\mathbf{W}$  and  $\mathbf{H}$  were initialized by the rough estimates of the ECG and EMG reshaped spectrograms with fixed cut-off frequencies (Fig.1b). This is basically the same procedure as in *Step 1* (filtering + decimation), followed by the NMF algorithm (1) – (5) with  $r = 1$ . Observe that the ECG additionally undergoes spectral whitening by means of the linear prediction analysis of order 5, which is meant to further suppress the residual EMG energy at low frequencies. According to Fig.1b, *Step2* provides two sets of matrices ( $\mathbf{W}_{\text{ECG}} \mathbf{H}_{\text{ECG}}$ ) and ( $\mathbf{W}_{\text{EMG}} \mathbf{H}_{\text{EMG}}$ ) which are merged into initial  $\mathbf{W}$  and  $\mathbf{H}$ .

*Step3.* In the last step (Fig.1c) the NMF algorithm (1) – (5) is performed on the reshaped input spectrogram with the

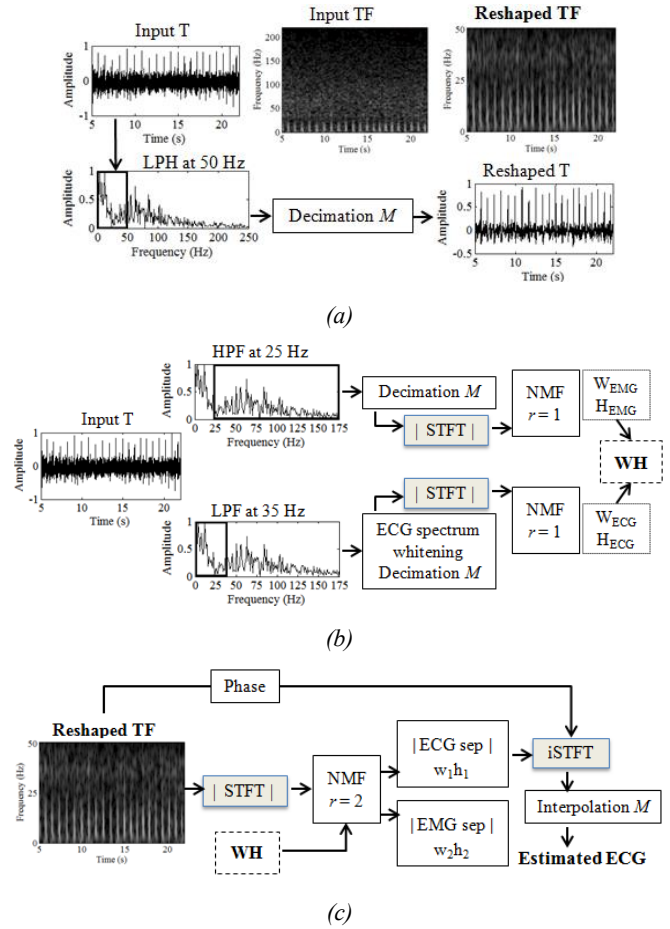


Fig. 1. Proposed method: (a) reshaping the input spectrogram, (b) calculating the initial  $\mathbf{W}$  and  $\mathbf{H}$  and (c) NMF analysis.

previously obtained initial  $\mathbf{W}$  and  $\mathbf{H}$  matrices and  $r = 2$  (two signal sources are expected). The estimated spectrogram of ECG is transformed back into the time domain by means of the inverse STFT. The phase information required by this transform is obtained by assuming that at each STFT sample one of the underlying sources is dominant [9]. Finally, interpolation of the obtained ECG waveform was performed with factor  $M$  set in such a way to recover the original sampling rate.

### III. RESULTS

In this section, the efficiency of the proposed approach will be evaluated through a comparative study. The comparison reference methods are: a Butterworth filter [1] and the method based on wavelets and ICA approach (further denoted as WICA) [5]. The former is a popular 4<sup>th</sup> order Butterworth filter with the cut-off frequency set to 30 Hz. The latter uses the ECG–EMG spectral differences for component discrimination. It combines nonlinearly scaled wavelets and ICA (FastICA) to remove the ECG contribution to the EMG in a low-frequency band where both components overlap heavily. This method, however, provides significantly different outputs for the same input settings.

Accordingly, we have taken into account only the best quality separation results.

### A. Synthetic signals

The input signals are generated by mixing synthetic ECG and EMG signals. The ECG signal was generated with the MATLAB simulation program [14]. The P, Q, R, S, and T wave properties were given the default values, while the mean heart rate was set to 1.2 Hz. The EMG component was created following a general approach described in [2, 15], i.e. by passing a zero-mean unitary-variance Gaussian white noise through an all-poles bandpass filter with filter coefficients: [1, 1.9408, 1.3108, -0.2965, -0.0037, 0.0588]. The ECG and EMG components are mixed together according to the chosen signal-to-noise (SNR) ratio level, where signal/noise refers to the ECG and EMG respectively.

In order to generate the spectrograms, the following settings have been used: signal duration = 10 s, original sampling frequency  $f_s = 1000$  Hz, decimation/interpolation factor  $M = 10$ , window type = Hanning, analysis window size = 0.24 s with 50% overlap.

The performance comparison was carried out in the following way. The SNR was varied in the range -8 dB to 8 dB with 4 dB step. For each SNR, we evaluated the methods 100 times and calculated the estimated averaged ECG. Since the original sources are available, the quality of separation could be evaluated by Signal-to-Residual Ratio (SRR) defined as:

$$SRR[dB] = 10 \log_{10} \frac{\sum_n S_{ECG}(n)^2}{\sum_n [S_{ECG}(n) - \hat{S}_{ECG}(n)]^2} \quad (6)$$

where  $S_{ECG}(n)$  and  $\hat{S}_{ECG}(n)$  are the original and estimated ECG components. The last expression is the energy ratio of the original signal and the error between the original and separated signal expressed in decibels. The performance curves  $SRR = SRR(SNR)$  are shown in Fig.2.

We observe in all performance curves a general trend of ascending SRR towards larger SNR. This is not surprising, as we expected all the methods to perform well in situations of low-impact EMG. The filter and WICA method exhibit a similar performance, although the filter method is slightly better, particularly at higher SNR where it is situated around 3 dB over the WICA. For low SNR both methods undergo important performance degradation, due to the EMG energy increase within the ECG frequency band. Consequently, more EMG energy is retained by the filter, while the wavelet analysis in the WICA fails to properly localize the ECG components in the TF plain. The proposed method clearly outperforms the reference methods in the whole analysis range, and in particular at low SNR. For instance, with  $SNR = -8$  dB it achieves a SRR of about 10 dB over the reference methods.

The methods were also tested beyond analysis range. For SNR lower than -8dB, dominating EMG source made separation impossible for all of the methods. In case of SNR higher than 8 dB, the proposed method performed worse not only because ECG component was dominating over EMG in T domain but also in reshaped TF spectrum.

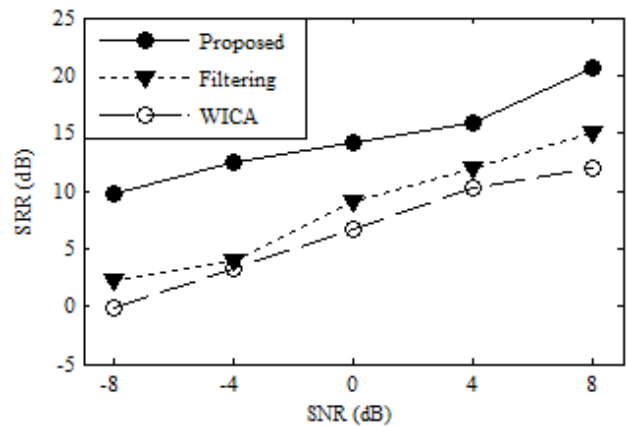


Fig. 2. SRR versus SNR for the methods involved in the comparative study.

### B. Real signals

The experimental procedure was conducted in accordance with the Declaration of Helsinki and was approved by the Local Ethics Committee. Each subject provided an informed written consent before participation in the study. The experimental session was performed with a KinCom Isokinetic Dynamometer (Chattanooga, TN, USA). The subjects performed two maximal voluntary contractions (MVC) of right knee extension over a period of 5 s, separated by 2 min of rest. The highest MVC value was used to obtain the submaximal force levels. After 2 min of rest, the subjects were asked to maintain an isometric right-knee extension at 30% and at 80% MVC for as long as possible. EMG activity during the isometric contraction of the vastus medialis of the right leg was recorded using a grid of 65 surface electrodes (5 columns  $\times$  13 electrodes; 2.5 mm interelectrode distance). The grid was placed along the direction of the muscle fibers, between the innervations zone and the distal tendon, previously identified during a preliminary brief knee isometric contraction. A reference electrode was placed around the right ankle. Before the placement of the electrodes, the skin was shaved, lightly abraded and cleaned with water. The signals were amplified as monopolar derivations (EMG amplifier, LISiN-OT Bioelettronica, Torino, Italy), band-pass filtered (-3 dB bandwidth, 1-500 Hz), sampled at 2048 samples/s, and converted to digital data by a 12-bit A/D converter board.

For the proposed method the following settings have been used: signal duration = 5 s, original sampling frequency  $f_s = 2048$  Hz, decimation/interpolation factor  $M = 20$ , window type = Hanning, analysis window size = 0.46 s with 50% overlap. The performance comparison was carried out for two subjects with different MVC (30% and 80%). For real signals, the use of SRR was not possible, as the signal components before the mixture were not available. Thus, only a graphical comparison is shown.

The comparison results in the form of time-domain signals are shown in Fig.3 and Fig.4 for MVC = 30% and MVC = 80% respectively. In both figures the subfigure (a) shows the input signal, while the subfigures (b - d) represent the estimated ECG component for the WICA, filtering and proposed method respectively.

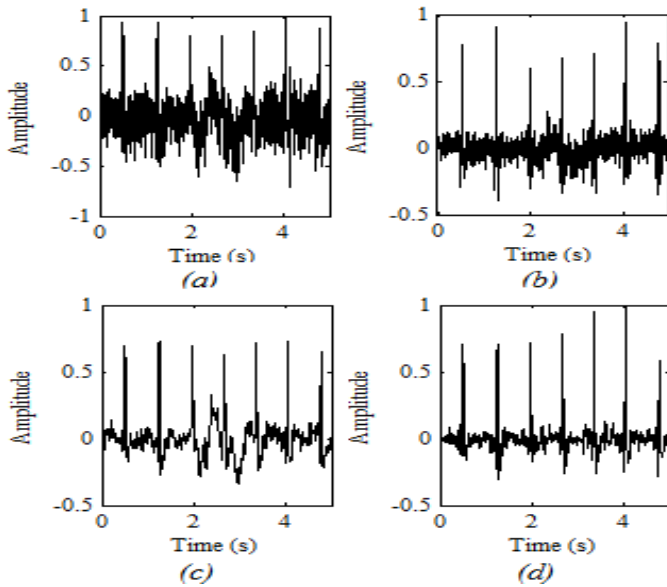


**Fig. 3.** (a) Input signal for the subject with MVC 30%, (b) estimated ECG for the WICA, (c) estimated ECG for the filtering and (d) estimated ECG for the proposed method.

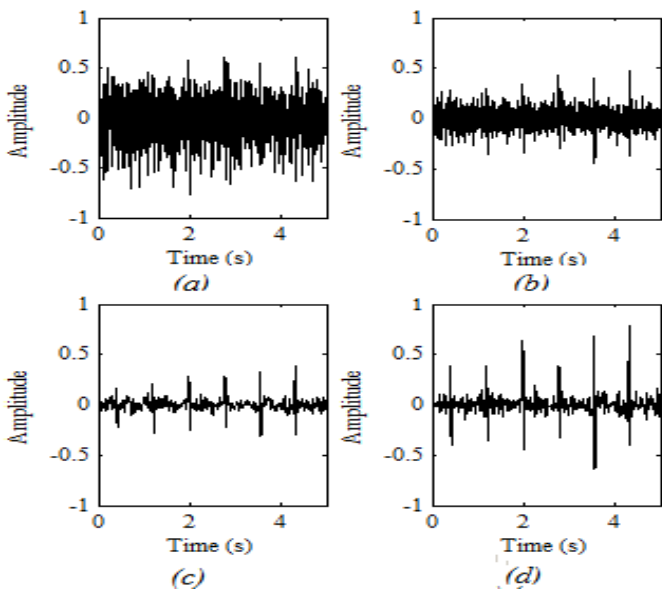


**Fig. 4.** (a) Input signal for the subject with MVC 80%, (b) estimated ECG for the WICA, (c) estimated ECG for the filtering and (d) estimated ECG for the proposed method.

Visual inspection of Fig.3 and Fig.4 brings out the impact of each method on the ECG-EMG separation. In both cases the WICA retains most of the EMG residual energy in the estimated ECG, while the filtering and proposed methods are clearly better, which is in accordance with Fig.2. In addition, observe that the low-frequency movement artifact around  $t = 2.5$  s could not be removed by neither the WICA nor filtering method. The proposed method, on the contrary, efficiently pulls it out of the mixture, thus yielding an artifact-free ECG signal. Moreover, note that the proposed method can adequately deal with very-low-SNR scenarios

(Fig.4) as it provides the estimated ECG with the sharpest QRS complexes.

#### REFERENCES

- [1] M. S. Redfern, R. E. Hughes, and D. B. Chaffin, "High-pass filtering to remove electrocardiographic interference from torso EMG recordings", *Clin. Biomech.*, vol. 8, pp. 44–48, 1993.
- [2] Y. Deng, W. Wolf, and R. Schnell, "New aspects to event-synchronous cancellation of ECG interference: An application of the method in diaphragmatic EMG signals," *IEEE Trans. Biomed. Eng.*, vol. 47, no. 9, pp. 1177–1184, Sep. 2000.
- [3] G. Lu, J. Brittain, P. Holland, J. Yianni, A. Green, J. Stein, T. Aziz, and S. Wang, "Removing ECG noise from surface EMG signals using adaptive filtering," *Neurosci. Lett.*, vol. 462, no. 1, pp. 14–19, Oct 2009.
- [4] C. Marque, C. Bisch, R. Dantas, S. Elayoubi, V. Brosse, and C. Perot, "Adaptive filtering for ECG rejection from surface EMG recordings," *J. Electromyogr. Kinesiol.*, vol. 15, no. 3, pp. 310–315, Jun. 2005.
- [5] V. von Tscherner, B. Eskofier, and P. Federolf, "Removal of the electrocardiogram signal from surface EMG recordings using nonlinearly scaled wavelets," *J. Electromyogr. Kinesiol.*, vol. 21, no. 4, pp. 683–688, Aug. 2011.
- [6] J. Mak, Y. Hu, and K. Luk, "An automated ECG-artifact removal method for trunk muscle surface EMG recordings," *Med. Eng. Phys.*, vol. 32, no. 8, pp. 840–848, Oct. 2010.
- [7] P. Smaragdis and J. Brown. "Non-negative matrix factorization for polyphonic music transcription." In *IEEE Workshop on Applications of Signal Processing to Audio and Acoustics (WASPAA'03)*, pages 177–180, Oct. 2003.
- [8] T. Virtanen, "Monaural sound source separation by non negative matrix factorization with temporal continuity and sparseness criteria," *IEEE Trans. on Audio, Speech and Language Processing*, vol. 15, no. 3, pp. 1066–1074, 2007.
- [9] T. Virtanen, PhD Thesis "Sound Source Separation in Monaural Music Signals", Tampere University of Technology, 2006.
- [10] H. Lee, A. Cichocki, and S. Choi, "Nonnegative matrix factorization for motor imagery EEG classification," in *Proceedings of the International Conference on Artificial Neural Networks*. Athens, Greece: Springer, 2006.
- [11] Y. Yazama, Y. Mitsukura, M. Fukumi, N. Akamatsu, "Recognition from EMG Signals by an Evolutional Method and Non-negative Matrix Factorization" *Lecture Notes in Computer Science 2773*, pp. 594-600, 2003.
- [12] D. Lee and H. S. Seung, "Learning the parts of objects by non-negative matrix factorization", *Nature*, 401:788–791, 1999.
- [13] D. Lee and H. S. Seung, "Algorithms for non-negative matrix factorization", In V. T. Todd Leen, Tom Dietterich, editor, *Advances in Neural Information Processing Systems 13*, pages 556-562. MIT Press, Cambridge, MA, 2001.
- [14] R. Karthik, ECG simulation using Matlab. [Online].
- [15] C. Zhan, L. F. Yeung, and Z. Yang, "A wavelet-based adaptive filter for removing ECG interference in EMGdi signals," *J. Electromyogr. Kinesiol.* no. 20, pp. 542–549, 2010.